

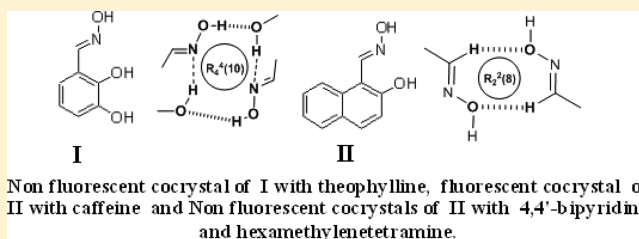
Solution and Solid State Study on the Recognition of Hydroxyaromatic Aldoximes by Nitrogen Containing Compounds

Arup Tarai and Jubaraj B. Baruah*

Department of Chemistry, Indian Institute of Technology Guwahati, Guwahati 781 039, Assam, India

Supporting Information

ABSTRACT: Structural aspects and fluorescence behaviors of a series of cocrystals of hydroxyaromatic aldoximes, namely, $2(\text{H}_2\text{NAP}) \cdot (4,4'\text{-bipyridine})$, $2(\text{H}_2\text{NAP}) \cdot (\text{HMTA})$, $\text{H}_2\text{NAP} \cdot \text{caffeine}$, and $(\text{H}_3\text{OHPA}) \cdot \text{theophylline} \cdot 2\text{H}_2\text{O}$, where $\text{H}_3\text{OHPA} = 2,3\text{-dihydroxyphenylaldoxime}$, $\text{H}_2\text{NAP} = 2\text{-hydroxynaphthaldoxime}$, $\text{HMTA} = \text{hexamethylenetetramine}$, were studied. A difference in fluorescence behavior of oxime molecules in solution and solid states was observed. The $\text{H}_2\text{NAP} \cdot \text{caffeine}$ cocrystals are fluorescence active in the solid state but not in solution. The combinations of H_3OHPA and $4,4'\text{-bipyridine}$, HMTA or caffeine in the solid state did not yield cocrystals; however, these combinations in solution caused fluorescence quenching of H_3OHPA . On the other hand, a hydrated cocrystal of H_3OHPA with theophylline, namely, $(\text{H}_3\text{OHPA}) \cdot \text{theophylline} \cdot 2\text{H}_2\text{O}$, was isolated and characterized. It was found that this combination causes fluorescence quenching of $2,3\text{-dihydroxyphenylaldoxime}$ (H_3OHPA) in the solution state but not in the solid state as a cocrystal. The fluorescence change of H_3OHPA interacting with theophylline can be identified among several aldoximes such as $2\text{-hydroxynaphthaldoxime}$ (H_2NAP), $2\text{-hydroxyphenylaldoxime}$ (H_2PA), and $2,4\text{-dihydroxyphenylaldoxime}$ (H_3PHPA). The synthons involved in each cocrystal are identified, and the fluorescence emission differences leading to molecular recognition are determined. The differences in fluorescent behavior among aldoximes were exploited for their identification and separation.



INTRODUCTION

The chromophoric molecule in the solid state can be stacked by the formation of cocrystals in a systematic manner to rationally alter luminescence properties.¹ Jones and co-workers² had shown that the fluorescence properties of face-to-face stacked arrangements guided by weak aromatic interactions of chromophoric compounds can be tuned by cofomers. On the basis of extensive studies, it was also suggested that the orientation and stacking patterns of chromophoric units in a crystal structures influence the luminescence of organic materials.^{3–5} A frequently occurred problem in tuning fluorescence emissions has been to obtain a suitable packing pattern that dictates the emission process.⁶ Strongly self-interacting systems, namely, pyrene and its derivatives in the solid state, generally show low fluorescence efficiencies due to such effects. However, these problems can be overcome by cocrystal formation with cofomers.⁶ There are also examples of anthrylpyrazole derivatives which show anthracene arrangement dependent emissions in the solid state.⁷ Further, the aggregation due to stacking and related weak interactions can influence the fluorescence emission in different compounds.^{8–10} Because of the difference in the fluorescence property of a component of molecule in a cocrystal, there is ample scope to study such properties in solid or in solution to bring out diversity in applications. The fluorescence properties associated with hydroxyaromatic oximes to sense nerve gas as shown by Rebek and co-workers^{11–13} and the utilities of such compounds in the detection of chemical warfare reagents as

shown by Anslyn and co-workers^{14–16} project them as an important class of molecules needing attention from solid state studies. Aakeroy's group^{17–20} has established various synthons of oximes and their cocrystals. Moreover, available green synthetic methods for the preparation of oximes have added a new flavor with future prospects.^{21,22} Recently, we have shown various assemblies of oximes generated by fluoride ions.²³ The pioneering research of Desiraju on the concept of synthons²⁴ made a big impact in crystal engineering,^{25–27} and having said this aromatic aldoximes have a large scope to serve as one of the basis to study varieties of hydrogen bonded assemblies.²⁸

Because of the directional nature of hydrogen bonds, there is a large scope for different orientations of hydroxyaromatic aldoximes or in their host–guest complexes in the solid state to construct new synthons.²⁹ Generally aldoximes form assemblies having $R_2^2(8)$ homosynthon^{21,22} as shown in Figure 1a, but introducing a hydroxy group to the aromatic aldoximes such as in $2\text{-hydroxyphenylaldoxime}$ (H_2PA) changes self-assemblies, and in this particular case $R_4^4(10)$ type heterosynthon as illustrated in Figure 1b was observed.³⁰ Thus, it would be of interest to know about synthons present in polyaromatic aldoximes and polyhydroxyaromatic aldoximes, as such compounds would differ in packing patterns due to the presence of the polyaromatic rings or the additional hydroxy groups. Two such

Received: July 20, 2015

Revised: November 14, 2015

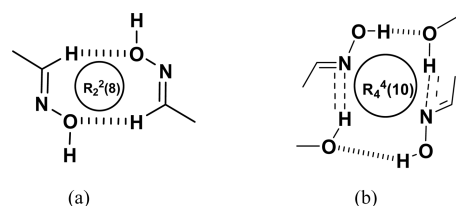


Figure 1. (a) Homosynthon observed in aldoximes and (b) heterosynthon observed in 2-hydroxyphenylaldoxime (H₂PA).

examples are 2-hydroxynaphthaldoxime (H₂NAP) and 2,3-dihydroxyphenylaldoxime (H₃OHPA) for which different possibilities of arranging hydroxy groups as shown in Figure 2a,b exist. In this study we have explored the structures of these

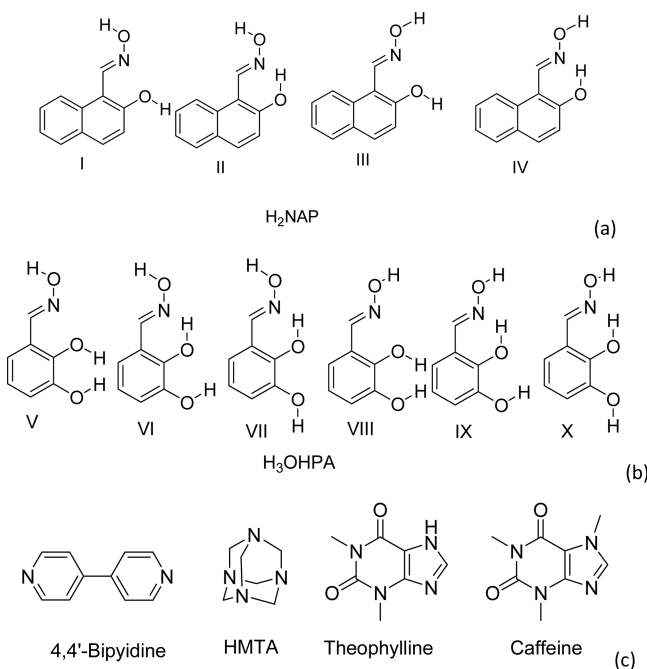


Figure 2. Orientations of active hydrogen atoms in (a) 2-hydroxynaphthaldoxime and (b) 2,3-dihydroxyphenylaldoxime. (c) Coformers 4,4'-bipyridine, hexamethylenetetramine (HMTA), theophylline, and caffeine.

two compounds and also their cocrystals with a series of nitrogen containing heterocyclic molecules (Figure 2c) that are of general interest in crystal growth. We also correlated the fluorescence properties in solid and solution states for molecular recognition in these combinations.

RESULTS AND DISCUSSION

The H₂NAP was found to be a good cofomer and accordingly from different solutions of H₂NAP and 4,4'-bipyridine or hexamethylenetetramine (HMTA) or caffeine 2:1 molar ratios were allowed to crystallize, and the respective cocrystal was crystallized. H₂NAP formed a 2:1 cocrystal with 4,4'-bipyridine or HMTA. But the cocrystal formed with caffeine was in a 1:1 ratio of H₂NAP and caffeine. The theophylline molecule has a close structural similarity with caffeine. Theophylline has an N–H bond to form hydrogen bond, but H₂NAP failed to yield a cocrystal with theophylline. In this case the parent compounds were recovered upon slow evaporation. ¹H NMR spectra of parent compounds and cocrystals were recorded, and

fluorescence studies in solution were carried out to see if such selectivity in interactions can be obtained in the solution state too. To understand if any change in the chemical shift of the protons of the oxime molecules takes place it was essential to record a 2D HOMOCOSY of the oxime molecules so as to clearly assign the aromatic peaks through the correlation (cross peaks). From the correlation shown in Supporting Figure 1S (H₂NAP) and 2S (H₃OHPA), we arrived at the assignment of each peak on the aromatic ring. The respective solution of the cocrystal did not show any change in the ¹H NMR chemical shifts of the protons on the oxime (Supporting Figures 3S–6S). Fluorescence emissions of the H₂NAP and cocrystals in solution and solid state are discussed under a separate heading to explain structural relationships.

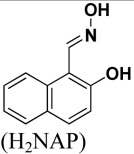
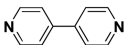
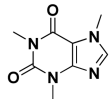
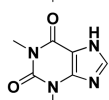
Attempts were made to prepare cocrystals of H₃OHPA with theophylline or caffeine under analogous conditions used for obtaining cocrystals of H₂NAP with caffeine. Only a cocrystal between H₃OHPA and theophylline was obtained, but no cocrystal between H₃OHPA and caffeine was observed. In addition to these the slow evaporation of methanol solutions of oximes such as H₂PA and H₃OHPA with the cofomers, namely, 4,4'-bipyridine or hexamethylenetetramine or caffeine or theophylline, did not yield any cocrystals, but precipitation of the respective parent compounds was observed in each case.

The fluorescence behaviors of the cocrystals in solid are different from the solution of the similar combinations, which are listed in Table 1. To understand these observations, a systematic structural study and consequences of packing in their optical properties was examined.

Structural Study. Analysis of the structure of the H₃OHPA has shown that it has R₄⁴(10) O–H_{aldoxime}⋯O–H_{hydroxy} heterosynthons similar to the heterosynthons found in the structure of the H₂PA.³⁰ The self-assembly of the compound has an intramolecular hydrogen bond of O–H of the 2-hydroxy group with the nitrogen atom of the oxime as illustrated in Figure 3a. The dimeric self-assembly of the H₃OHPA has two O–H⋯O interactions to stabilize a 10-member ring. The crystal structure of H₂NAP was reported earlier;³¹ it forms a dimeric self-assembly by two C–H⋯O interactions to construct an eight-member ring as illustrated in Figure 3b. The self-assembly of the H₂NAP is comprised of R₂²(8) type homosynthons, which has C–H⋯O interactions. Such synthons are common in aldoximes.^{17–20} In this case, an intramolecular hydrogen bond between the hydroxy group and the nitrogen atom of oxime was observed. From the stability point of the synthons observed in the case of H₃OHPA and H₂NAP, the former has higher stability for obvious reasons for the hierarchy of the bond strength between the O–H⋯O interaction over a C–H⋯O interaction.

Slow evaporation of the respective solution (in methanol, dimethyl sulfoxide, acetonitrile, ethanol, etc.) of H₃OHPA with 4,4'-bipyridine or HMTA or caffeine or theophylline yielded crystals from only one of these combinations, namely, from the solution of H₃OHPA with theophylline. This cocrystal was a dihydrate of a 1:1 cocrystal between H₃OHPA and theophylline. Self-assembly of this cocrystal is formed through hydrogen bonds with the water molecules to hold the oxime and cofomer molecules. While forming self-assemblies as shown in the Figure 4a, the dimeric assemblies that were present in the packing pattern of the parent structure of the H₃OHPA were disrupted. In the cocrystal each aldoxime molecule forms water assisted assemblies with theophylline. One O–H bond of water molecule hydrogen bonds with the carbonyl oxygen atom of

Table 1. Different Cocrystals of Oximes and Fluorescence Properties

Coformer	Fluorescence behaviour ^a	Fluorescence behaviour ^b
 (H ₂ NAP)	In solid-state	In solution
 2 : 1 cocrystal 2(H ₂ NAP).(4,4'-bipyridine)	Non-fluorescent	No cocrystal was obtained
 2 : 1 cocrystal 2(H ₂ NAP).(HMTA)	Non-fluorescent	No cocrystal was obtained
 1:1 cocrystal H ₂ NAP.caffeine	Fluorescent	No cocrystal was obtained
 No cocrystal was obtained	---	1:1:2 cocrystal ^c H ₃ OHPA.theophylline.water

^aIn solution no change. ^bNo cocrystal was obtained, hence solid state fluorescence not measured. ^cNonfluorescent in solid.

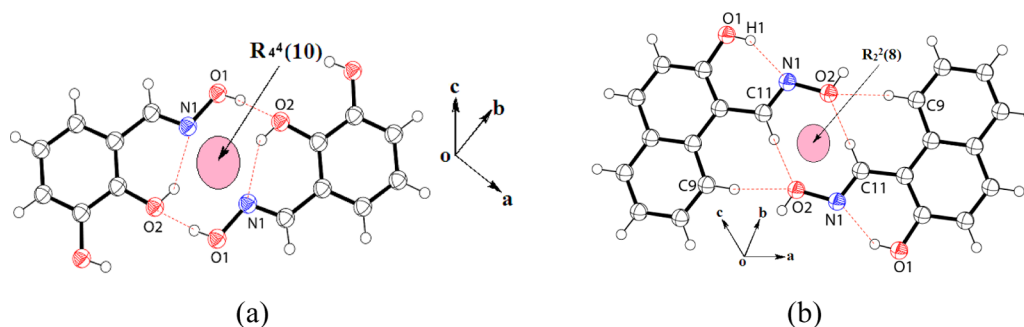


Figure 3. Dimeric assemblies of the compounds (a) H₃OHPA and (b) H₂NAP.

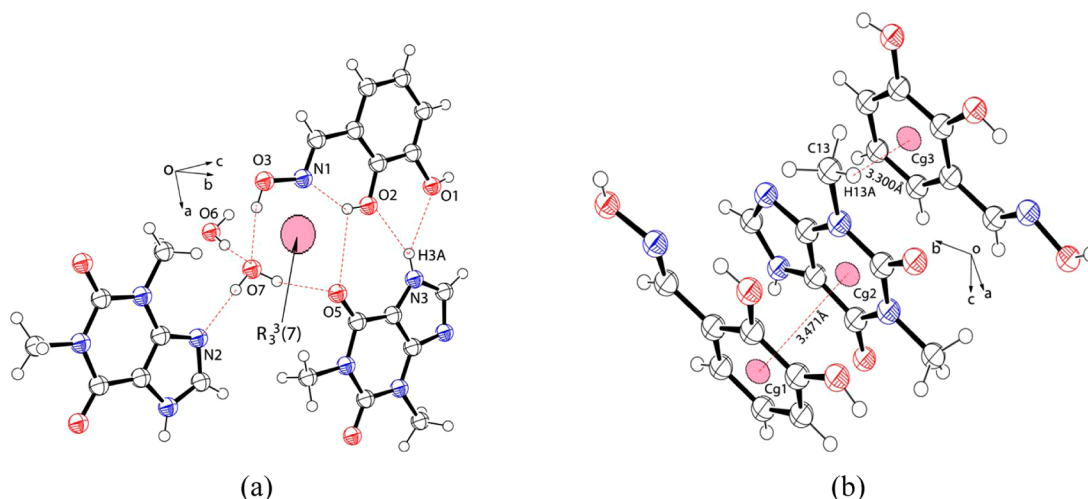


Figure 4. (a) Self-assemblies of hydrated cocrystal of H₃OHPA with theophylline. (b) π - π interactions between oxime and coformer.

theophylline and the oxygen atom of the same water molecule connects to the oxime O–H bond of the H₃OHPA. The carbonyl group of theophylline is involved in a bifurcated hydrogen bond by connecting the phenolic O–H group present at the 2-position of the aromatic ring. These

interactions yield a R₃³(7) motif, which holds the key to form the cocrystal of three components. The orientation of the active hydrogen atoms of oxime in this cocrystal is different with respect to the orientations observed in the parent oxime without a coformer. The parent oxime molecule adopts the

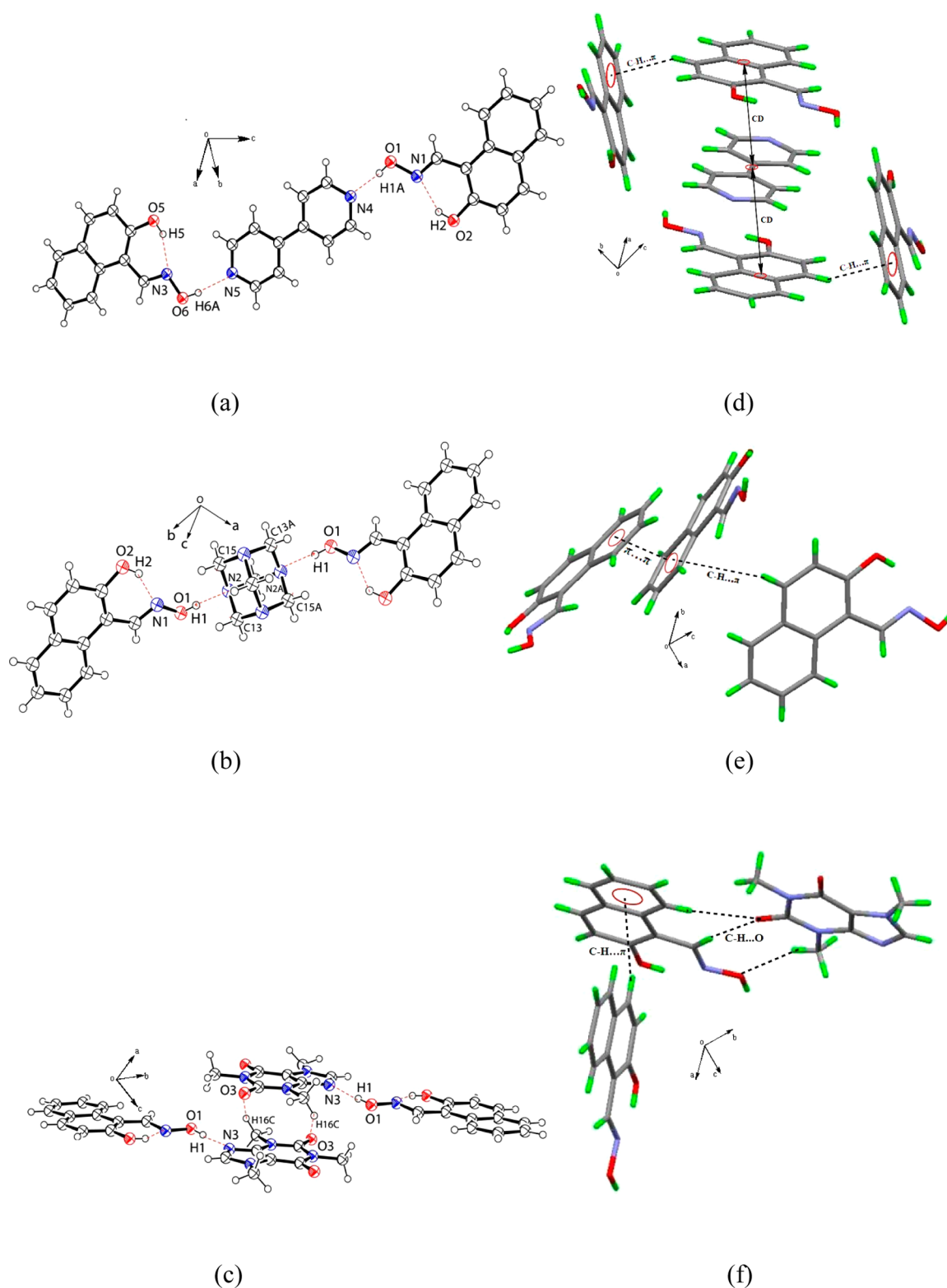


Figure 5. Structures of cocrystals of H₂NAP with (a) 4,4'-bipyridine, (b) HMTA, and (c) caffeine. (d–f) Different weak interactions present in the packing patterns of the three cocrystals.

orientation IX of the Figure 2, but the orientation X shown in the Figure 2 is observed in the cocrystal. An interesting feature of this cocrystal is the stacking interactions between theophylline and oxime molecules. The molecules show π -stacking (Figure 4b) between the rings with a separation distance 3.471 Å, which is conducive to strong π - π interactions.⁶ This

interaction originates from the dipolar nature of the theophylline molecule which has an electron deficient ring to interact with the electron rich ring of H₃OHPA.

After attempted crystallization of various solutions of H₂NAP and 4,4'-bipyridine or HMTA or caffeine or theophylline, cocrystals were obtained from three out of four such

independent combinations. Accordingly cocrystals $2(\text{H}_2\text{NAP}) \cdot (4,4'\text{-bipyridine})$ or $2(\text{H}_2\text{NAP}) \cdot (\text{HMTA})$ or $\text{H}_2\text{NAP} \cdot \text{caffeine}$ were isolated but attempts to get cocrystals from the solutions of H_2NAP with theophylline failed. The precipitate obtained from the solution of H_2NAP and theophylline was analyzed by a conventional technique (powder X-ray diffraction, PXRD,) and found that the precipitate was composed of just a physical mixture of two components. This confirmed that there was no cocrystal formation in this particular case. The interesting feature is that the cocrystals of H_2NAP with 4,4'-bipyridine or HMTA had a 2:1 molar ratio of oxime to coformer, whereas with caffeine it was a 1:1 cocrystal. It may be mentioned that polymorphic forms and solvates of caffeine with anthrallinic acid was reported in the literature;³² moreover same host molecule can form cocrystals with caffeine and theophylline differing in molar ratios.³³ Water bridged assemblies in the cocrystals of caffeine or theophylline were also reported.³⁴ Hence in anticipation of hydrated cocrystals in the present study the powder XRD patterns of the bulk samples of the cocrystals were examined to ascertain their phase purity (Figures 7S–8S). All the cocrystals of H_2NAP reported in this study are found to be anhydrous, and no solvated cocrystals were observed from any of the solvents used for crystallization. But the cocrystal of H_3OHPA with theophylline is a dihydrate. The structures of the cocrystals of H_2NAP with 4,4'-bipyridine or HMTA possesses similar $\text{O} \cdots \text{H} \cdots \text{N}$ interactions as shown in Figure Sa,c, but the packing patterns widely differ. Packing patterns are guided by $\text{O} \cdots \text{H} \cdots \text{N}$, $\text{C} \cdots \text{H} \cdots \text{O}$, and $\text{C} \cdots \text{H} \cdots \pi$ interactions in the cocrystals with 4,4'-bipyridine, but in the case of the HMTA cocrystal, the packing pattern is guided by $\text{O} \cdots \text{H} \cdots \text{N}$, $\text{C} \cdots \text{H} \cdots \text{O}$, $\text{C} \cdots \text{H} \cdots \pi$, and $\pi \cdots \pi$ interactions. Here $\pi \cdots \pi$ interactions play a crucial role in distinguishing the packing patterns of these two cocrystals.

Parent H_2NAP has an orientation II shown in Figure 2, whereas in the cocrystals the oxime part has structure of orientation I of Figure 2. In general the structures of the three cocrystals of H_2NAP may be suggested to be composed of H_2NAP molecules held by weak interactions with respective cofomers in two different ways. The first two cocrystals, namely, with H_2NAP with 4,4'-bipyridine or HMTA, are based on either a planar or a nonplanar bridging unit anchoring two guest molecules through $\text{O} \cdots \text{H} \cdots \text{N}$ hydrogen bonds, whereas the third cocrystal that is H_2NAP with caffeine has two stacked guest molecules holding two H_2NAP molecules (Figure 5c). The prominent weak interactions of these cocrystals are shown in Figure 5d–f, and the hydrogen bond parameters are given in the Table 1S.

The IR spectrum of H_2NAP has $\text{O} \cdots \text{H}$ stretching frequency at 3331 cm^{-1} . This peak shifts to a higher wavenumber in the case of each cocrystal and appears in the region $3445\text{--}3460 \text{ cm}^{-1}$. Such shifts are attributed to the formation of hydrogen bonds in the cocrystals through the oxime OH and nitrogen atom of the respective coformer. The $\text{O} \cdots \text{H}$ frequency of H_2NAP is shifted in cocrystals; it is 3445 cm^{-1} in the 4,4'-bipyridine cocrystal and 3446 cm^{-1} in the HMTA cocrystal, whereas it is at 3460 cm^{-1} in the cocrystal with caffeine. This trend is reflected in the $\text{O} \cdots \text{H} \cdots \text{N}$ bond parameters; the caffeine cocrystal has the higher donor–acceptor distance with the largest $\text{O} \cdots \text{H} \cdots \text{N}$ angle among the three cocrystals. The H_2NAP has $\text{C}=\text{N}$ stretching at 1632 cm^{-1} , and the cocrystals of H_2NAP show a characteristic $\text{C}=\text{N}$ bond stretching in the region of $1628\text{--}1658 \text{ cm}^{-1}$. This shows that the $\text{C}=\text{N}$ bond is intact in the cocrystals, and the nitrogen atom of this unit does

not participate in a strong hydrogen bond. The cocrystal $\text{H}_2\text{NAP} \cdot \text{caffeine}$ has a strong $\text{C}=\text{O}$ stretching at 1704 cm^{-1} from the carbonyl group of the caffeine part. A similar carbonyl stretching absorption in the IR spectra of the cocrystal $\text{H}_3\text{OHPA} \cdot \text{theophylline} \cdot 2\text{H}_2\text{O}$ appears at 1706 cm^{-1} .

Fluorescence Studies. To ascertain the suitable wavelengths for fluorescence excitation studies, UV-visible spectra of solid samples of each cocrystal were recorded. They show broad absorption in the region of $350\text{--}400 \text{ nm}$ originating from the host molecule. The broadening arises due to a proximity broadening effect from self-interacting molecules in the vicinity in solid samples. The absorbance peaks of individual oxime molecules and the corresponding cocrystals are given in the Supporting Figure 9S. On the basis of the observation on the UV–visible absorption shown by the oximes and cocrystals, the emission spectra in each case were investigated by exciting at 368 nm (Figure 6). The oxime H_2NAP exhibited a broad

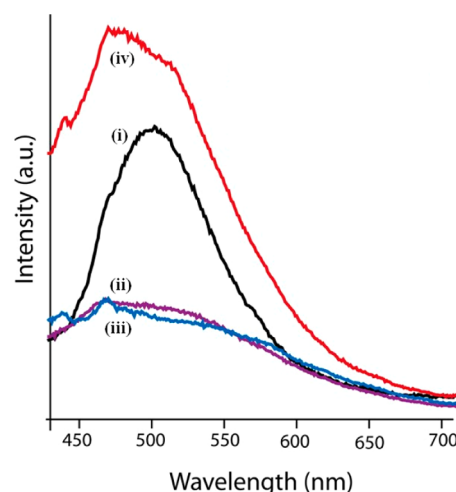


Figure 6. Solid state fluorescence emission spectra of the (i) H_2NAP , (ii) $2(\text{H}_2\text{NAP}) \cdot (4,4'\text{-bipyridine})$, (iii) $2(\text{H}_2\text{NAP}) \cdot (\text{HMTA})$, and (iv) $\text{H}_2\text{NAP} \cdot \text{caffeine}$ (excitation in each case at 368 nm).

emission band around $475\text{--}530 \text{ nm}$. The cocrystal of H_2NAP with caffeine showed a relatively higher fluorescence emission intensity with a shift toward a shorter wavelength, whereas the cocrystals of the H_2NAP with 4,4'-bipyridine or hexamethylenetetramine are weakly fluorescent. This suggests that upon cocrystal formation with 4,4'-bipyridine or HMTA the fluorescence of the H_2NAP gets quenched by the respective coformer. In these experiments uniformity in sample preparation was ensured by carrying out experiments with similar amounts, and the fluorescence was measured under identical conditions.

It is a well-known fact that fluorescence of organic compounds in the solid state depends on the architecture of crystal packing,³⁵ and $\pi \cdots \pi$ stacking interactions cause fluorescence quenching.⁶ On the other hand it was also suggested that $\text{C} \cdots \text{H} \cdots \pi$ interactions can contribute to fluorescence changes.⁶ Aggregation such as H-aggregate formed by assembling of the same type of molecules on top of each other results in shifting of fluorescence to shorter wavelength, whereas a J-aggregate does it in an opposite manner.³⁶ The difference of fluorescence in the present cocrystals illustrated in Table 2 can be attributed to the respective packing patterns. Close analyses of the structures of the H_2NAP and cocrystals have shown that self-assemblies of the oxime molecules are

Table 2. Characteristic Fluorescence Properties of H₂NAP and Cocrystals in the Solid State

compound/cocrystals	λ_{ab} (nm)	λ_{ex} (nm)	λ_{em} (nm)	quantum yields Φ_F
H ₂ NAP	390	368	510	0.052
H ₂ NAP·caffeine	395	368	468	0.095
2(H ₂ NAP)·(4,4'-bipyridine)	397	368	470	0.015
2(H ₂ NAP)·(HMTA)	395	368	470	0.014

guided by several weak interactions. The weak interactions like O–H...N, C–H...O, and O–H...O in the H₂NAP and cocrystals are shown in Figure 7a–d. The packing pattern of each cocrystal is different from the packing pattern observed in the parent oxime. From the crystal densities among these cocrystals (Table 3), the 4,4'-bipyridine cocrystal has a lower

crystal density than the HMTA cocrystal, and both have several weak interactions, but the latter has additional $\pi\cdots\pi$ interactions. Since the cocrystals H₂NAP with 4,4'-bipyridine and HMTA are in 1:2 molar ratio, this factor contributes to cause a large difference between the packing patterns of these two crystals with respect to the packing pattern of the cocrystal of H₂NAP with caffeine which has a 1:1 molar ratio of host and coformer. The caffeine molecules in the caffeine cocrystal are positioned on top of the oxime molecules, and the center core distance is 3.718 Å. The carbonyl group of caffeine molecule forms a hydrogen bond with oxime. The naphthalene unit of caffeine cocrystal is involved in C–H... π interaction with the neighboring naphthalene unit present in the lattice. To have effective $\pi\cdots\pi$ stacking interactions between two planar fluorophoric π -units, they should have a parallel arrangement, and each of the interacting rings must be positioned on top of each other, whereas to have a center-dot C–H... π interaction

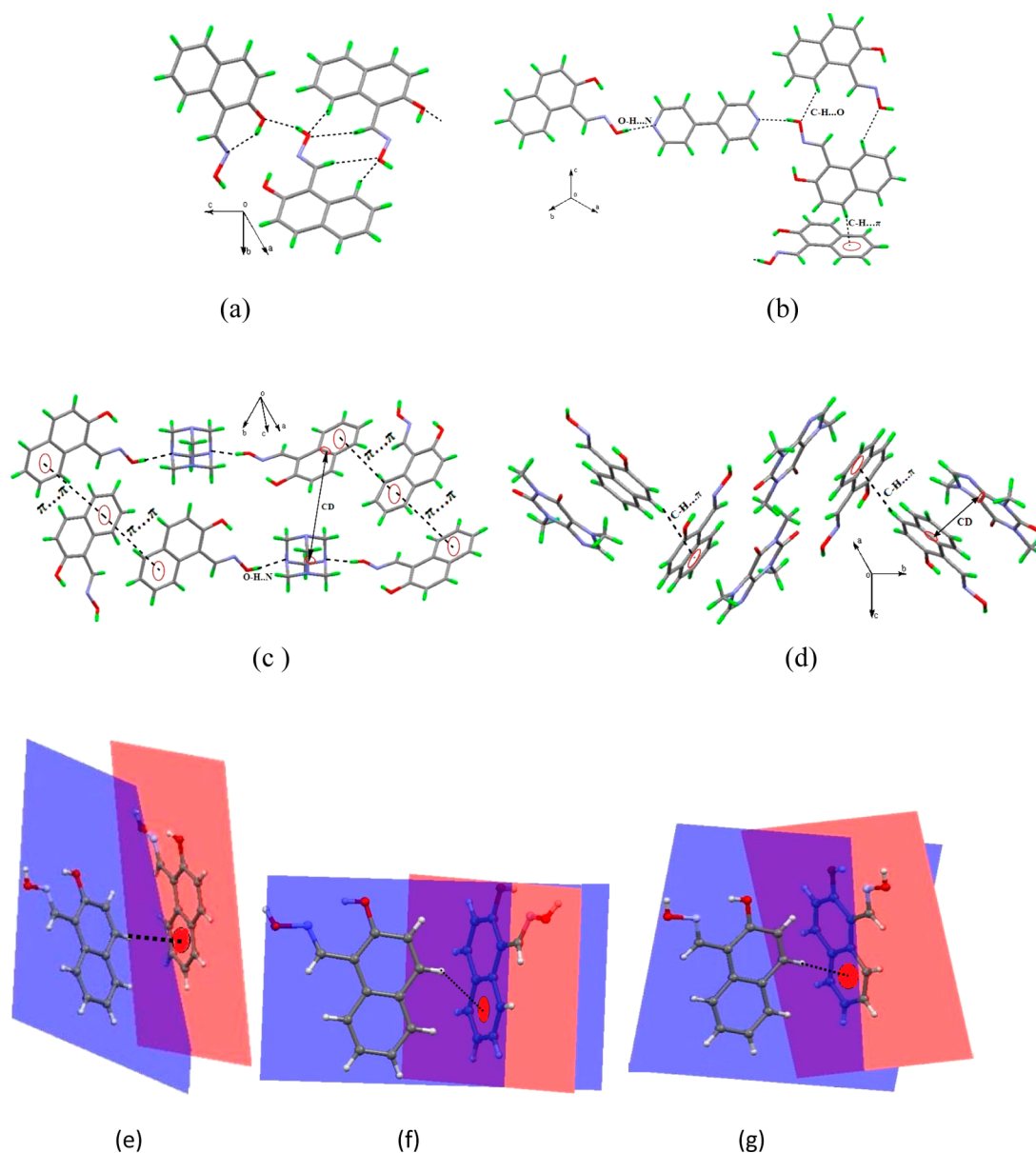


Figure 7. Packing diagram of (a) H₂NAP, (b) cocrystals 2(H₂NAP)·(4,4'-bipyridine), (c) cocrystals 2(H₂NAP)·(HMTA), (d) cocrystals H₂NAP·caffeine. The stacking of the fluorophoric H₂NAP in the cocrystal (e) (H₂NAP)₂·4,4'-bipyridine [$\angle 67.17^\circ$], (f) (H₂NAP)₂·HMTA [$\angle 76.06^\circ$], and (g) (H₂NAP)·caffeine [$\angle 86.12^\circ$]. In each case the angle between the planes of the H₂NAP is shown in the third bracket.

Table 3. Crystallographic Parameters of the Host and the Cocrystals

	H ₂ NAP (redetermined)	H ₃ OHPA	(H ₂ NAP) ₂ ·4,4'- bipy	(H ₂ NAP)·caffeine	(H ₂ NAP) ₂ · HMTA	H ₃ OHPA-theophylline· 2H ₂ O
formula	C ₁₁ H ₉ NO ₂	C ₇ H ₇ NO ₃	C ₃₂ H ₂₆ N ₄ O ₄	C ₁₉ H ₁₉ N ₅ O ₄	C ₁₄ H ₁₃ N ₃ O ₂	C ₁₄ H ₁₉ N ₃ O ₇
mol wt	187.19	153.14	530.57	381.39	257.29	369.34
space group	<i>P2₁/c</i>	<i>P2₁/c</i>	<i>P2₁/c</i>	<i>P2₁/c</i>	<i>Aba2</i>	<i>P2₁/n</i>
<i>a</i> (Å)	14.856(2)	11.211(10)	11.8301(5)	8.9467(9)	10.0199(5)	8.8538(8)
<i>b</i> (Å)	4.0568(6)	4.662(4)	14.4094(6)	25.487(3)	27.8962(17)	17.6944(15)
<i>c</i> (Å)	16.585(2)	14.146(12)	23.9854(10)	8.8264(9)	9.1641(6)	10.7717(10)
α (deg)	90.00	90.00	90.00	90.00	90.00	90.00
β (deg)	115.029(9)	111.793(17)	96.922(3)	114.334(6)	90.00	90.464(5)
γ (deg)	90.00	90.00	90.00	90.00	90.00	90.00
<i>V</i> (Å ³)	905.6(2)	686.5(10)	4058.9(3)	1833.8(3)	2561.5(3)	1687.5(3)
density, g cm ⁻³	1.373	1.482	1.302	1.381	1.334	1.454
abs coeff, mm ⁻¹	0.096	0.118	0.088	0.100	0.092	0.118
<i>F</i> (000)	392	320	1668	800	1088	776
total no. of reflections	1616	1173	7344	3335	2320	3040
reflections, <i>I</i> > 2 σ (<i>I</i>)	1147	599	3858	2709	1948	2308
max θ /°	25.24	25.25	25.25	25.25	25.24	25.24
ranges (<i>h</i> , <i>k</i> , <i>l</i>)	-17 ≤ <i>h</i> ≤ 16 -4 ≤ <i>k</i> ≤ 4 -19 ≤ <i>l</i> ≤ 19	-12 ≤ <i>h</i> ≤ 11 -5 ≤ <i>k</i> ≤ 5 -12 ≤ <i>l</i> ≤ 16	-13 ≤ <i>h</i> ≤ 14 -17 ≤ <i>k</i> ≤ 16 -28 ≤ <i>l</i> ≤ 28	-10 ≤ <i>h</i> ≤ 10 -24 ≤ <i>k</i> ≤ 30 -10 ≤ <i>l</i> ≤ 10	-7 ≤ <i>h</i> ≤ 7 -8 ≤ <i>k</i> ≤ 8 -15 ≤ <i>l</i> ≤ 15	-10 ≤ <i>h</i> ≤ 10 -20 ≤ <i>k</i> ≤ 21 -12 ≤ <i>l</i> ≤ 12
complete to 2 θ (%)	98.70	93.70	99.90	100.00	100.00	99.60
data/restraints/ parameters	1616/0/129	1173/0/103	7344/0/547	3335/0/258	2320/1/175	3040/4/256
GOF (<i>F</i> ²)	1.059	1.045	1.003	1.058	1.072	1.025
<i>R</i> indices [<i>I</i> > 2 σ (<i>I</i>)]	0.0414	0.0721	0.0481	0.0573	0.0384	0.0428
<i>wR</i> ₂ [<i>I</i> > 2 σ (<i>I</i>)]	0.0661	0.1577	0.1046	0.1794	0.1020	0.1338
<i>R</i> indices (all data)	0.0623	0.1337	0.1119	0.0704	0.0475	0.0575
<i>wR</i> ₂ (all data)	0.0718	0.1948	0.1317	0.1957	0.1094	0.1468

the interacting C–H of one ring should appear at a position which is perpendicular to the central point of the other ring. Thus, we examined the arrangements of the fluorophoric π -units, namely, H₂NAP in the cocrystals, and compared with the packing pattern of the H₂NAP. The angles between such planes are shown in Figure 7e–g. In the case of the caffeine cocrystal it is $\angle 86.12^\circ$, which is very close to a perpendicular arrangement and hence has the least $\pi\cdots\pi$ stacking interactions but has better C–H $\cdots\pi$ interactions among the others. On the other hand, the parent compound does not have similar C–H $\cdots\pi$ interactions, but the packing has rings at a slightly translated parallel position to each other, so that a highly effective $\pi\cdots\pi$ stacking interaction is not feasible. Further analysis of the other two cocrystals shows a less than 90° angle between the planes suggesting the positions of the rings to be nonparallel. However, the deviations from perpendicular positions are not enough to cut off the effective C–H $\cdots\pi$ interactions. Such qualitative analysis is not good enough to form an overall picture to explain the fluorescence changes. It can easily explain fluorescence changes in three cases leaving aside the 4,4'-bipyridine cocrystals as an exception. Complete segregation of H₂NAP molecules in the cocrystal with caffeine leads to monomer type arrangements to show emission with higher intensity with a slight blue shift. This may be compared to J-aggregate (H₂NAP) transformed to an arrangement of discrete monomers (H₂NAP in caffeine cocrystal).³⁶ The parent compound can be considered as a partially quenched state, and the π -stacking induced by the HMTA cocrystal causes quenching of the fluorescence in the case of the cocrystal with HMTA. To provide even a qualitative explanation of the solid state fluorescence property of the cocrystal with 4,4'-bipyridine, an explanation has to account for three symmetry independent host molecules, which is difficult;

nonetheless we can suggest with the data available from the experiments that parallel stacking of the pyridine ring of bipyridine units could be the major factor contributing to the quenching of fluorescence in this particular case.

To ascertain interactions between the H₂NAP with the cofomers in solution, the fluorescence emission spectra of solution of H₂NAP by adding cofomers were recorded. No changes in fluorescence emissions were observed by these cofomers. Hence these results suggest that dilute solution interactions between the respective cofomer and H₂NAP are too weak to detect. Similar results are reflected in the ¹H NMR titrations between selected cofomers with H₂NAP where no change in peak positions was observed (Figures S14–S15). These results clearly demonstrate that the optical properties of the compound H₂NAP is not affected by cofomers in solution but in solid cofomers play a major role to either enhance or reduce the intensities and positions.

The compound H₃OHPA is nonfluorescent, and its cocrystal with theophylline is also nonfluorescent in the solid state. But H₃OHPA shows fluorescence in solution, whereas the respective solution of compounds H₂NAP or H₃OHPA in dimethyl sulfoxide–water mixture has an emission peak at 395 and 387 nm upon excitation at 310 and 270 nm, respectively. The fluorescence emission of the H₃OHPA at 387 nm was gradually decreased upon addition of theophylline as shown in the Figure 8. Similar changes were also observed at pH = 3 and pH = 10 (Figure 10S). A relatively higher quenching effect was observed at pH = 3 as compared to pH = 10; hence it may be suggested that it is the exchange of hydrogen between the hydrogen bond donor and acceptor that holds the key to the quenching of fluorescence. The differences observed in fluorescence by theophylline have prompted us to take up

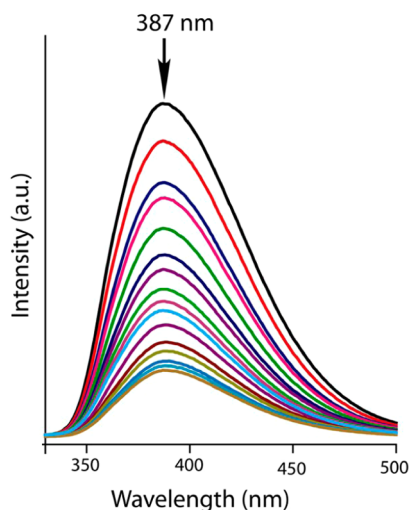


Figure 8. Changes in the fluorescence emission spectra of H₃OHPA (10⁻⁵ M solution in DMSO-H₂O) on addition of theophylline (10⁻⁵ M in DMSO-H₂O, 10 μL aliquot).

screening of aldoximes by theophylline. For this purpose fluorescence spectra of H₂NAP, H₃OHPA, H₃PHPA, and H₂PA (the latter two compounds were taken as screening compounds) were monitored by adding a solution of theophylline to the respective oxime solution. It was interesting to note that addition of theophylline to a respective solution of H₂NAP or H₂PA or H₃PHPA (Supporting Figures 11S–13S) did not cause fluorescence spectral changes. These oximes were not recognized by theophylline to cause changes in their respective emission spectra. We have also examined the effect on fluorescence emission of H₃OHPA by adding a solution of caffeine or 4,4'-bipyridine or HMTA; in each case fluorescence quenching was observed, but these compounds could not change the fluorescence emissions of the H₂NAP, H₂PA, and H₃PHPA. Even though all four cofomers resulted in fluorescence quenching of H₃OHPA in the solution state, only one of them (theophylline) formed a cocrystal. Hence the solution study clearly tells that careful choice of nitrogen aromatic compounds can screen a series of oximes to identify a particular oxime. Theophylline is the most important metabolite of caffeine, and it is found in tea, coffee, cocoa beans, and chocolate.³⁷ Theophylline forms cocrystal with phenols,^{38–41} carboxylic acids,^{42,43} and various other organic molecules.^{44,45} On the other hand, caffeine has the ability to form cocrystals with carboxylic acids⁴⁶ and nicotinamides.⁴⁷ Since the quenching process is very selective to H₃OHPA by cofomers; it is attributed to the effect of the 3-hydroxy group which is participating in proton transfer in this particular example. Three other examples of oximes lack a hydroxy group at the 3-position with respect to the oxime functional group of the aromatic ring. It may be noted that among the oximes H₂NAP, H₂PA, H₃PHPA, and H₃OHPA, H₃OHPA has the distinction of having a hydroxy group at the 3-position of the ring with respect to the oxime functional group. This hydroxy group is not in conjugation with the oxime functional group through the intervening π -electrons of the ring. This makes the fluorescence behavior of this oxime different from the other three oximes in the presence of cofomers in solution.

CONCLUSIONS

Two different hydrogen bonded cyclic motifs of the H₃OHPA and H₂NAP are modified by cofomers. In solution 4,4'-bipyridine, HMTA, and caffeine cause quenching of fluorescence of H₃OHPA, suggesting that interactions of these compounds with H₃OHPA involve the hydroxy group at the 3-position, whereas in the theophylline cocrystal all the hydrogen bonding sites are used, causing complete quenching of fluorescence. On the other hand, the cocrystals of H₂NAP with 4,4'-bipyridine or HMTA or caffeine were formed easily. π -Stacking plays the decisive role to increase or decrease fluorescence in the solid state of H₂NAP and cocrystals of H₂NAP. In solution no interactions of H₂NAP with cofomers were observed. By virtue of such properties different oximes can be distinguished by the fluorescence technique either in the solid state or in solution. The differences in fluorescent behavior among aldoximes could be exploited for their identification and separation.

EXPERIMENTAL SECTION

Synthesis and Characterization of the Oximes and Cocrystals. Oximes H₂NAP and H₃OHPA were prepared from their respective hydroxyaromatic aldehyde by reacting them with hydroxylamine hydrochloride in the presence of pyridine. A general procedure for the synthesis of 2-hydroxynaphthaldoxime (H₂NAP) and 2,3-dihydroxypenylaldehyde (H₃OHPA) is as follows: pyridine (1 mL) was added dropwise to a solution of hydroxylamine hydrochloride (0.138 g, 2 mmol) in ethanol (20 mL). The resulting solution was stirred at room temperature for 15 min, and respective aldehyde (2 mmol) was added. The solution was stirred at room temperature for 1 h. A yellow precipitate of compound H₂NAP or H₃OHPA was obtained. The entire reaction mixture was extracted with ethyl acetate and washed with water. The ethyl acetate layer was taken separately, and on removal of solvent by using a rotary evaporator yielded compound H₂NAP or H₃OHPA.

2-Hydroxynaphthaldoxime (H₂NAP). Melting point: 155–160 °C, isolated yield: 82%. ¹H NMR (400 MHz, DMSO-*d*₆): 11.53 (s, 1H), 9.04 (s, 1H), 8.48 (d, *J* = 8.4 Hz, 1H), 7.86 (d, *J* = 6.4 Hz, 1H), 7.84 (d, *J* = 6.4 Hz, 1H), 7.55 (t, *J* = 7.2 Hz, 1H), 7.41 (t, *J* = 6.8 Hz, 1H), 7.34 (d, 1H). IR (KBr, cm⁻¹): 3331 (br, m), 3013 (w), 2924 (w), 2766 (w), 1947 (w), 1758 (w), 1632 (s), 1591 (s), 1526 (w), 1464 (w), 1463 (m), 1414 (m), 1369 (w), 1310 (m), 1268 (s), 1239 (s), 1182 (s), 1163 (w), 1143 (w), 1079 (w), 1034 (w), 1014 (s), 938 (s), 878 (w), 854 (w), 814 (s), 776 (s), 744 (m), 718 (w), 649 (w), 541 (w), observed mass (ESI) *m/z*: 188.0698 (M + 1); (calculated exact mass for (M + H) 188.0712 for C₁₁H₁₀NO₂).

2,3-Dihydroxypenylaldehyde (H₃OHPA). Melting point: 115–120 °C, isolated yield: 83%. ¹H NMR (400 MHz, DMSO-*d*₆): 11.30 (s, 1H), 9.58 (s, 1H), 9.27 (s, 1H), 8.31 (s, 1H), 6.91 (d, *J* = 7.2 Hz, 1H), 6.66 (d, *J* = 7.6 Hz, 1H), 6.59 (t, *J* = 8 Hz, 1H). IR (KBr, cm⁻¹): 3454 (br), 1620 (s), 1592 (w), 1478 (s), 1444 (m), 1412 (w), 1347 (m), 1308 (m), 1285 (m), 1251 (m), 1165 (s), 1075 (m), 1030 (s), 967 (s), 850 (s), 782 (s), 744 (m), 727 (m), 626 (s), 566 (w). Observed mass (ESI) *m/z*: 154.1049. (Calculated exact mass for M + H 154.0504 for C₇H₈NO₃).

Cocrystals were obtained by slow evaporation of a solution of the respective aldoxime and the guest molecules with respective molar ratio in methanol.

(H₂NAP)₂·4,4'-bipyridine. Isolated yield: 76%. ¹H NMR (600 MHz, DMSO-*d*₆): 11.52 (s, 1H), 11.14 (s, 1H), 9.03 (s, 1H), 8.72 (d, *J* = 5.4 Hz, 3H), 8.47 (d, *J* = 8.4 Hz, 1H), 7.85 (m, 4H), 7.50 (t, *J* = 7.2 Hz, 1H), 7.35 (t, *J* = 6.8 Hz, 1H), 7.20 (d, *J* = 9, 1H). IR (KBr, cm⁻¹): 3445 (bs), 1631 (s), 1596 (s), 1537 (w), 1467 (m), 1405 (m), 1369 (w), 1344 (w), 1307 (m), 1276 (s), 1239 (s), 1215 (s), 1183 (m), 1161 (w), 1145 (w), 1080 (w), 1062 (w), 1038 (s), 1023 (m), 999 (m), 940 (s), 880 (w), 825 (s), 799 (s), 776 (w), 744 (m), 671 (w), 645 (w), 620 (s).

(H₂NAP)₂·HMTA. Isolated yield: 78%. ¹H NMR (600 MHz, DMSO-*d*₆): 11.50 (s, 1H), 11.10 (s, 1H), 9.03 (s, 1H), 8.47 (d, *J* = 8.4 Hz, 1H), 8.00 (s, 1H), 7.85 (t, *J* = 8 Hz, 2H), 7.51 (t, *J* = 7.2 Hz, 1H), 7.37 (t, *J* = 6.8 Hz, 1H), 7.20 (d, *J* = 9 Hz, 1H), 4.55 (s, 12H). IR (KBr, cm⁻¹): 3446 (bs), 2959 (w), 2924 (w), 2875 (w), 1628 (m), 1591 (s), 1525 (w), 1464 (s), 1424 (w), 1370 (m), 1348 (w), 1312 (s), 1276 (s), 1238 (s), 1227 (s), 1180 (m), 1163 (w), 1144 (w), 1083 (w), 1007 (s), 947 (w), 933 (s), 870 (m), 825 (w), 813 (s), 800 (s), 738 (s), 723 (m), 693 (s), 673 (m), 665 (m), 644 (m).

(H₂NAP)·caffeine. Isolated yield: 82%. ¹H NMR (600 MHz, DMSO-*d*₆): 11.50 (s, 1H), 11.10 (s, 1H), 9.03 (s, 1H), 8.47 (d, *J* = 8.4 Hz, 1H), 8.00 (s, 1H), 7.85 (t, *J* = 8.4 Hz, 2H), 7.51 (t, *J* = 7.2 Hz, 1H), 7.37 (t, *J* = 6.8 Hz, 1H), 7.20 (d, *J* = 9 Hz, 1H), 3.87 (s, 3H), 3.41 (s, 3H), 3.21 (s, 3H). IR (KBr, cm⁻¹): 3460 (bs), 3003 (w), 2922 (w), 1704 (s), 1658 (s), 1593 (w), 1553 (s), 1496 (s), 1468 (m), 1407 (w), 1362 (w), 1326 (m), 1282 (s), 1240 (s), 1211 (w), 1181 (s), 1140 (w), 1037 (m), 1022 (m), 978 (w), 938 (s), 878 (w), 829 (s), 780 (m), 757 (w), 744 (s), 669 (m), 645 (m), 607 (m).

(H₃OHPA)·theophylline·2H₂O. Isolated yield: 86%. ¹H NMR (600 MHz, DMSO-*d*₆): 11.29 (s, 1H), 9.56 (s, 1H), 9.25 (s, 1H), 8.30 (s, 1H), 8.02 (s, 1H), 6.91 (d, *J* = 7.2 Hz, 1H), 6.79 (d, *J* = 8.4 Hz, 1H), 6.68 (t, *J* = 7.8 Hz, 1H), 3.44 (s, 3H), 3.23 (s, 3H). IR (KBr, cm⁻¹): 3479 (s), 3218 (bs), 1706 (s), 1650 (s), 1558 (s), 1505 (s), 1465 (w), 1440 (w), 1421 (w), 1385 (m), 1315 (m), 1259 (s), 1232 (s), 1190 (s), 1099 (w), 1058 (m), 994 (s), 959 (w), 933 (m), 849 (m), 780 (m), 764 (m), 741 (s), 711 (w), 654 (w), 620 (w), 505 (s).

Physical Measurements. Powder X-ray diffraction patterns were recorded using Bruker powder X-ray diffractometer D2 phaser. Infrared spectra of the solid samples were recorded on a PerkinElmer Spectrum-One FT-IR spectrophotometer in the region 4000–400 cm⁻¹ by making KBr pellets. Mass spectra were recorded on a micro mass Q-TOF (waters) mass spectrometer by using an acetonitrile/formic acid matrix. Solution state UV–visible spectra were recorded using PerkinElmer Lambda-750 spectrometer. Solid state UV–visible spectra were recorded by the same equipment using the diffuse reflectance technique by taking the respective powdered sample in a solid sample holder. Fluorescence emissions were measured in a PerkinElmer LS-55 spectrofluorimeter by taking a definite amount of solutions of samples and exciting them at required wavelengths. Solid state fluorescence spectra were recorded using a PerkinElmer LS-55 spectrofluorimeter by taking constant amounts of finely powdered samples. Solid fluorescence quantum yields (Φ_F) were measured using a Quanta-φ accessory. X-ray single crystal diffraction data for the cocrystals and 2,3-dihydroxypenylalldoxime (H₃OHPA) were collected at 298 K with Mo Kα radiation (λ = 0.71073 Å) with the use of a Bruker Nonius SMART APEX CCD diffractometer equipped with a graphite monochromator and an Apex CCD camera, whereas for the 2-hydroxynaphthaldoxime (H₂NAP) data were collected on a Oxford SuperNova diffractometer where the data refinement and cell reductions were carried out by CrysAlisPro. Data reduction and cell refinement were performed using SAINT and XPREP software. Multiscan empirical absorption corrections were carried out with the help of face-indexing. Structures were solved by direct methods using SHELXS-97 and were refined by full-matrix least-squares on F² using SHELXL-97. All the non-hydrogen atoms were refined in anisotropic approximation against F² of all the reflections. The hydrogen atoms were placed at their calculated positions and refined in the isotropic approximation. In the case of H₃OHPA-theophylline·2H₂O the hydrogen atoms on the water molecules were fixed. Crystallographic data collection was done at room temperature, and data are tabulated in Table 3.

■ ASSOCIATED CONTENT

Supporting Information

The Supporting Information is available free of charge on the ACS Publications website at DOI: 10.1021/acs.cgd.5b01375.

The ¹HNMR and PXRD of the cocrystals and various fluorescence titrations (PDF)

Accession Codes

CCDC 1417714–1417718 contains the supplementary crystallographic data for this paper. These data can be obtained free of charge via www.ccdc.cam.ac.uk/data_request/cif, or by emailing data_request@ccdc.cam.ac.uk, or by contacting The Cambridge Crystallographic Data Centre, 12, Union Road, Cambridge CB2 1EZ, UK; fax: +44 1223 336033.

■ AUTHOR INFORMATION

Corresponding Author

*Fax: +91-361-2690762; phone +91-361-2582311; e-mail: juba@iitg.ernet.in; Web: <http://www.iitg.ernet.in/juba>.

Notes

The authors declare no competing financial interest.

■ ACKNOWLEDGMENTS

The authors thank Ministry of Human Resource and Development for providing financial facilities to the Department of Chemistry Indian Institute of Technology, Guwahati.

■ REFERENCES

- (1) Wuest, J. D. *Nat. Chem.* **2012**, *4*, 74–75.
- (2) Yan, D.; Delori, A.; Lloyd, G. O.; Friscic, T.; Day, G. M.; Jones, W.; Lu, J.; Wei, M.; Evans, D. G.; Duan, X. *Angew. Chem., Int. Ed.* **2011**, *50*, 12483–12486.
- (3) Mizobe, Y.; Tohnai, N.; Miyata, M.; Hasegawa, Y. *Chem. Commun.* **2005**, *14*, 1839–1841.
- (4) Zhang, G. Q.; Lu, J. W.; Sabat, M.; Fraser, C. L. *J. Am. Chem. Soc.* **2010**, *132*, 2160–2162.
- (5) Zhou, T. L.; Jia, T.; Zhao, S. S.; Guo, J. H.; Zhang, H. Y.; Wang, Y. *Cryst. Growth Des.* **2012**, *12*, 179–184.
- (6) Feng, Q.; Wang, M.; Dong, B.; Xu, C.; Zhao, J.; Zhang, H. *CrystEngComm* **2013**, *15*, 3623–3629.
- (7) Zhang, Z.; Zhang, Y.; Yao, D.; Bi, H.; Javed, I.; Fan, Y.; Zhang, H.; Wang, Y. *Cryst. Growth Des.* **2009**, *9*, S069–S076.
- (8) Wagner, B. D.; McManus, G. J.; Moulton, B.; Zaworotko, M. J. *Chem. Commun.* **2002**, *18*, 2176–2177.
- (9) Lee, E. Y.; Jang, S. Y.; Suh, M. P. *J. Am. Chem. Soc.* **2005**, *127*, 6374–6381.
- (10) Kupcewicz, B.; Malecka, M. *Cryst. Growth Des.* **2015**, *15*, 3893–3904.
- (11) Dale, T. J.; Rebek, J., Jr. *J. Am. Chem. Soc.* **2006**, *128*, 4500–4501.
- (12) Dale, T. J.; Rebek, J., Jr. *Angew. Chem., Int. Ed.* **2009**, *48*, 7850–7852.
- (13) Kerkines, I. S. K.; Petsalakis, I. D.; Theodorakopoulos, G.; Rebek, J., Jr. *J. Phys. Chem. A* **2011**, *115*, 834–840.
- (14) Wallace, K. J.; Fagbemi, R. I.; Folmer-Andersen, F. J.; Morey, J.; Lynth, V. M.; Anslyn, E. V. *Chem. Commun.* **2006**, *37*, 3886–3888.
- (15) Wallace, K. J.; Morey, J.; Lynch, V. M.; Anslyn, E. V. *New J. Chem.* **2005**, *29*, 1469–1474.
- (16) Hewage, H. S.; Wallace, K. J.; Anslyn, E. V. *Chem. Commun.* **2007**, *38*, 3909–3911.
- (17) Aakeroy, C. B.; Beatty, A. M.; Leinen, D. S. *Cryst. Growth Des.* **2001**, *1*, 47–52.
- (18) Aakeroy, C. B.; Epa, K. N.; Forbes, S.; Desper, J. *CrystEngComm* **2013**, *15*, 5946–5949.
- (19) Sinha, A. S.; Epa, K. N.; Chopade, P. D.; Smith, M. M.; Desper, J.; Aakeroy, C. B. *Cryst. Growth Des.* **2013**, *13*, 2687–2695.
- (20) Bruton, E. A.; Brammer, L.; Pigge, F. C.; Aakeroy, C. B.; Leinen, D. S. *New J. Chem.* **2003**, *27*, 1084–1094.
- (21) Aakeroy, C. B.; Sinha, A. S.; Epa, K. N.; Spartz, C. L.; Desper, J. *Chem. Commun.* **2012**, *48*, 11289–11291.
- (22) Aakeroy, C. B.; Sinha, A. S. *RSC Adv.* **2013**, *3*, 8168–8171.
- (23) Tarai, A.; Baruah, J. B. *CrystEngComm* **2015**, *17*, 2301–2309.

- (24) Desiraju, G. R. *Angew. Chem., Int. Ed. Engl.* **1995**, *34*, 2311–2327.
- (25) Dey, A.; Kirchner, M. T.; Vangala, V. R.; Desiraju, G. R.; Mondal, R.; Howard, J. A. K. *J. Am. Chem. Soc.* **2005**, *127*, 10545–10559.
- (26) Sarma, J. A. R. P.; Desiraju, G. R. *Cryst. Growth Des.* **2002**, *2*, 93–100.
- (27) Thakur, T. S.; Desiraju, G. R. *Cryst. Growth Des.* **2008**, *8*, 4031–4044.
- (28) Salmon, D. J.; Smith, M. M.; Desper, J.; Aakeroy, C. B. *Cryst. Growth Des.* **2006**, *6*, 1033–1042.
- (29) Etter, M. C. *Acc. Chem. Res.* **1990**, *23*, 120–126.
- (30) Wood, P. A.; Forgan, P. A.; Henderson, D.; Parsons, S.; Pidcock, E.; Tasker, P. A.; Warren, J. E. *Acta Crystallogr., Sect. B: Struct. Sci.* **2006**, *62*, 1099–1111.
- (31) Guo, Z.; Li, L.; Liu, G.; Dong, J. *Acta Crystallogr., Sect. E: Struct. Rep. Online* **2008**, *64*, o568–o569.
- (32) Madusanka, N.; Eddleston, M. D.; Arhangel'skis, M.; Jones, W. *Acta Crystallogr., Sect. B: Struct. Sci., Cryst. Eng. Mater.* **2014**, *70*, 72–80.
- (33) Jacobs, A.; Noa, F. M. A. *CrystEngComm* **2015**, *17*, 98–106.
- (34) Das, B.; Baruah, J. B. *Cryst. Growth Des.* **2011**, *11*, 278–286.
- (35) Kupcewicz, B.; Malecka, M. *Cryst. Growth Des.* **2015**, *15*, 3893–3904.
- (36) Spano, F. C. *Acc. Chem. Res.* **2010**, *43*, 429–439.
- (37) Jafari, M. T.; Rezaei, B.; Javaheri, M. *Food Chem.* **2011**, *126*, 1964–1970.
- (38) Schultheiss, N.; Roe, M.; Boerrigter, S. X. M. *CrystEngComm* **2011**, *13*, 611–619.
- (39) Wang, Z.-L.; Wei, L.-H. *Acta Crystallogr., Sect. E: Struct. Rep. Online* **2007**, *63*, o1681–o1682.
- (40) Chatteraj, S.; Shi, L.; Sun, C. C. *CrystEngComm* **2010**, *12*, 2466–2472.
- (41) Sarma, B.; Saikia, B. *CrystEngComm* **2014**, *16*, 4753–4765.
- (42) Das, B.; Baruah, J. B. *Cryst. Growth Des.* **2011**, *11*, 278–286.
- (43) Abourahma, H.; Urban, J. M.; Morozowich, N.; Chan, B. *CrystEngComm* **2012**, *14*, 6163–6169.
- (44) Aitipamula, S.; Wong, A. B. H.; Chow, P. S.; Tan, R. B. H. *CrystEngComm* **2014**, *16*, 5793–5801.
- (45) Delori, A.; Galek, P. T. A.; Pidcock, E.; Patni, M.; Jones, W. *CrystEngComm* **2013**, *15*, 2916–2928.
- (46) Karki, S.; Friscic, T.; Jones, W.; Motherwell, W. D. S. *Mol. Pharmaceutics* **2007**, *4*, 347–354.
- (47) Lu, J.; Rohani, S. *Org. Process Res. Dev.* **2009**, *13*, 1269–1275.